

**NASA  
Technical  
Paper  
1991**

March 1982

# Friction and Surface Chemistry of Some Ferrous-Base Metallic Glasses

Kazuhisa Miyoshi  
and Donald H. Buckley

NASA  
TP  
1991  
c.1

0068153



TECH LIBRARY KAFB, NM

ALCOAN COPY: RETURN TO  
AFWL TECHNICAL LIBRARY  
KIRTLAND AFB, N. M.

**NASA**

**NASA  
Technical  
Paper  
1991**

1982

TECH LIBRARY KAFB, NM



0068153

# Friction and Surface Chemistry of Some Ferrous-Base Metallic Glasses

Kazuhisa Miyoshi  
and Donald H. Buckley  
*Lewis Research Center  
Cleveland, Ohio*

**NASA**

National Aeronautics  
and Space Administration

Scientific and Technical  
Information Branch

## Summary

Sliding friction experiments were conducted in argon and vacuum with ferrous-base metallic glasses. The objective of the investigation was to determine the friction and wear characteristics of the metallic glasses in both the amorphous and crystalline states. Experiments in vacuum were conducted at temperatures to 350° C with both as-received and ion-sputter-cleaned surfaces. XPS (X-ray photoelectron spectroscopy) was used to characterize surface chemistry. The experiments in argon were conducted with the alloy in the as-received and heat-treated conditions. The heat treatment was done to achieve crystallization. Three different slider materials—aluminum oxide, copper, and 52100 bearing steel—were used in contact with the metallic glasses. The surfaces were examined both dry and lubricated with mineral oil.

The results of the investigation indicate that crystallization of the alloys increases the coefficient of friction. Boric and silicon oxides were observed on the surfaces of these metallic glasses as a result of diffusion. Such segregation can influence friction behavior. Different ferrous-base metallic glasses have markedly different friction characteristics.

## Introduction

A host of different classes of materials are used in mechanical components wherein adhesion, friction, wear, and lubrication are involved. The single most significant class of these materials is metallic alloys. As a result, considerable research has been conducted to determine the effect of various properties of metallic alloys on tribological behavior.

In 1960 it was shown that by very rapid quenching of certain alloy compositions from the melt, amorphous solid phases could be formed (ref. 1). This discovery launched a new field of research activity. There are now well over 200 alloy systems that have been identified as being capable of quenching into the amorphous state (ref. 1). These alloys are referred to as metallic glasses (refs. 2 and 3).

Amorphous alloys (metallic glasses) are currently finding increased application in the aerospace industry (ref. 4). They are used for joining internal assemblies in gas turbines. Nickel-based brazing filler metals of the BNi classification are replacing the gold-based BAu-4

primarily for economic reasons. However, like BAu-4, the nickel-based filler metals have excellent flow behavior, are compatible with most stainless steels and nickel alloys, and offer an outstanding combination of high-temperature strength, fatigue properties, and oxidation and corrosion resistance (ref. 4). The braze foils are now used for many engine valves and other components. Amorphous metal is also becoming important as a magnetic material for highly developed magnetic recording devices (e.g., video tape recorders). In most high-density devices, a magnetic head in sliding contact with a magnetic tape is used for recording and playback. Therefore the magnetic head and tape must have good wear resistance. Ferrous-base amorphous alloys are attracting attention for use as magnetic heads as well as magnetic media. Amorphous alloys can also be used in foil bearings.

From a tribological point of view these amorphous alloys, or metallic glasses, have some very interesting properties. They are as hard as standard steels, yet unlike silicate glasses they possess substantial plasticity, are among the strongest known engineering materials, and resist the propagation of cracks. Their tribological behavior has not as yet been studied.

The objective of this investigation was therefore to determine the influence of the amorphous state of certain metallic alloys on tribological characteristics. Sliding friction experiments were conducted with three ferrous-base metallic glass compositions, both lubricated and unlubricated, in vacuum and argon. Riders of aluminum oxide, copper, and bearing steel were made to slide on the metallic glass surfaces under loads of 0.01 to 0.25 N and at sliding velocities of 0.033 to 0.17 mm/sec. The vacuum experiments were conducted at temperatures of 25° to 800° C. Comparative experiments were made with 304 stainless steel. This practical material was of equivalent foil thickness to the metallic glasses.

## Materials

Three metallic glass compositions were examined in this investigation. These compositions and some of their properties are presented in table I. The alloys were foils (0.05 mm thick) and except for heat treatments were used in the as-cast condition. The riders that were made to slide on the foils were single-crystal aluminum oxide (sapphire), 99.999-percent-pure copper, and 52100 bearing steel. The mineral oil used for lubrication was a pharmaceutical grade that had been degassed.

TABLE I. - PROPERTIES OF METALLIC GLASSES (REF. 2)

Alloy composition	Crystallization temperature, °C	Density, f/cm <sup>3</sup>	Hardness, GPa	Ultimate tensile strength, GPa	Bend ductility, <sup>a</sup> $\epsilon$
Fe <sub>67</sub> Co <sub>18</sub> B <sub>14</sub> Si <sub>1</sub>	430	7.56	10	1.5	1
Fe <sub>81</sub> B <sub>13.5</sub> Si <sub>3.5</sub> C <sub>2</sub>	450	7.3	10.3	.7	$9 \times 10^{-3}$
Fe <sub>40</sub> Ni <sub>38</sub> Mo <sub>4</sub> B <sub>18</sub>	410	8.02	10.5	1.38	1

<sup>a</sup> $\epsilon = t/(d - t)$ , where  $t$  is ribbon thickness and  $d$  is micrometer spacing at bend fracture.

## Apparatuses

Two apparatuses were used in this investigation. One was an ultra-high-vacuum system capable of measuring adhesion, load, and friction and containing an XPS spectrometer (fig. 1). Figure 1 indicates the major components, including the electron energy analyzer; the X-ray source, and the ion gun used for ion sputter etching. The X-ray source contained a magnesium anode. The specimens were mounted on the end of the specimen probe at an angle of 90° from the analyzer axis. The X-ray source was located at an angle of 79° from the analyzer axis. A manipulator-mounted beam was projected into the vacuum chamber. The beam contained two flats machined normal to each other with strain gages mounted thereon. The pin was mounted on the end of the beam. The load was applied by moving the beam normal to the flat and was sensed by strain gages. The vertical sliding motion of the pin along the flat surface was accomplished through a motorized manipulator assembly. The friction force under an applied load was measured during vertical translation by a strain gage mounted normal to that used to measure load.

The second apparatus used in this investigation is shown schematically in figure 2. It was basically a pin or rider on a flat. The samples were mounted on hardened steel flats and retained in a vice mounted on a screw-driven platform. The platform was driven through the screw by an electric motor with a gearbox that allowed for changing the sliding velocity. Motion was reciprocal. The rider was made to traverse a distance of 1 cm on the surface of the foil. A switch then reversed the direction of motion so that the rider retraced the original track from the opposite direction. This process was continuously repeated.

The rider was loaded against the foil with deadweights. The arm retaining the rider contained strain gages to measure the tangential and normal forces. The arm containing the rider could be moved normal to the direction of the wear tracks. Thus multiple tracks could be generated on a single surface. The entire apparatus

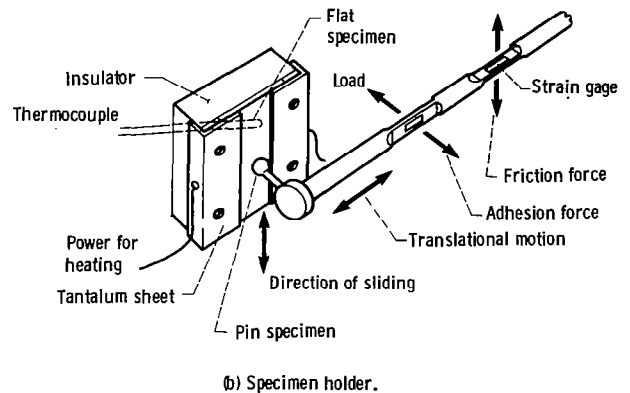
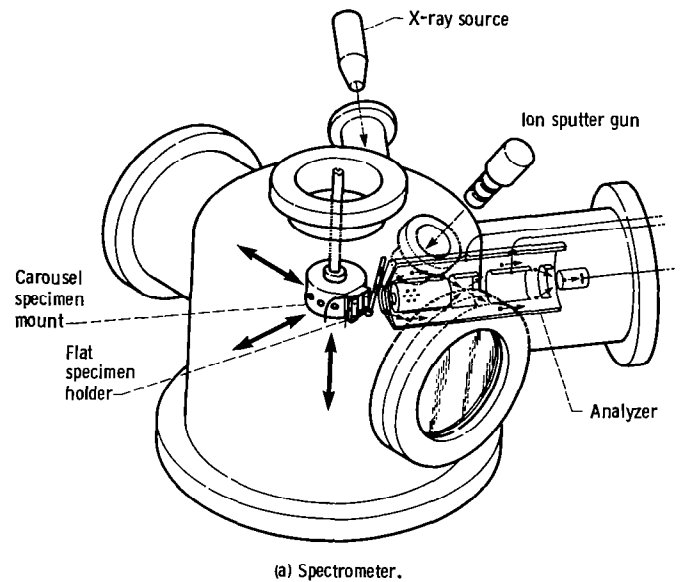


Figure 1. - Schematic representation of the x-ray photoelectron spectrometer and ultra-high-vacuum friction and wear apparatus.

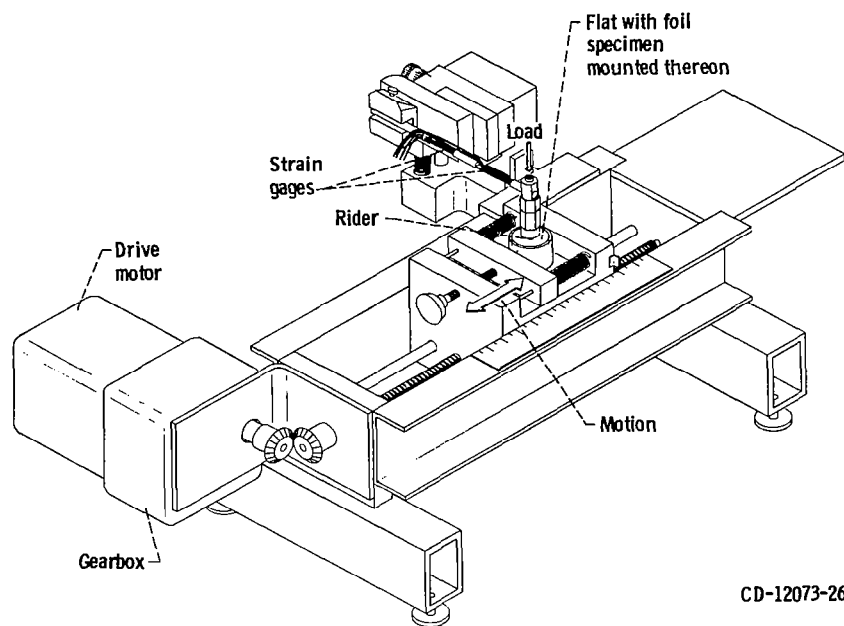


Figure 2. - Friction and wear apparatus.

was housed in a plastic box. The atmosphere in the box was controlled.

## Experimental Procedure

### Specimen Preparation and Heating

The foil specimen was attached to the insulator flat with tantalum supporting sheets (fig. 1). The specimen was directly in contact with the sheets. The flat and pin surfaces were rinsed with 200-proof ethyl alcohol just before they were placed in the vacuum chamber. After the specimens were placed in the vacuum chamber (fig. 1), the system was evacuated and then baked out at 250° C to obtain a pressure of 30 nPa ( $2 \times 10^{-10}$  torr) or lower.

The specimen was heated to 80° C during bakeout. Both flat and pin specimens were ion sputter cleaned. Before ion sputter etching the chamber pressure was 30 nPa ( $2 \times 10^{-10}$  torr) or lower, and the ion gun was outgassed for 2 min at 20 mA.

The titanium sublimation pump was operated for 2 min at 48 A. The ion pumps were then shut off. The inert gas argon was admitted into the system through a leak valve to the desired pressure, 8 mPa ( $5 \times 10^{-5}$  torr). Ion sputter etching was performed with a 3000-eV, 20-mA beam at an argon pressure of 8 mPa. The ion beam was continuously rastered over the specimen surface. After sputter etching the system was reevacuated to 30 nPa or lower, and the surface was then examined by XPS.

Heat treatment was next conducted in situ, and this included heating to a maximum temperature of 350° C

for 30 minutes at 10 nPa. The foil was resistance heated. XPS spectra were obtained at room temperature both before and after heating. The electric power for resistance heating of the specimen was supplied through the tantalum sheets. The temperature was measured with a type K (Ni-Cr vs. Ni-Al) thermocouple in direct contact with the specimen.

### Chemical Analysis of Surface

The XPS technique is very useful in providing analysis of the first few atomic layers of a specimen surface. The ultimate sensitivity is sufficient to allow fractions of a monolayer to be detected and identified. Both qualitative and quantitative information can be obtained with XPS because all of the elements in the periodic table above helium and its adjacent elements are clearly distinguished. There are not enough occupied energy levels in hydrogen and helium for detection.

To obtain reproducible results, a strict standardization of the order and time of recording was used, and the instrument was regularly calibrated by assuming the binding energy for the gold  $4f_{7/2}$  peak to be 83.8 eV. All survey spectra (scans of 1050 or 1100 eV) were taken at a pass energy of 50 or 100 eV, providing an instrumentation resolution of 1 eV. The magnesium  $K\alpha$  X-ray source was used with an X-ray source power of 400 W (10 kV, 40 mA). The narrow scans of the  $C_{1s}$ ,  $Si_{2p}$ ,  $O_{1s}$  were just wide enough to encompass the peaks of interest with a pass energy of 25 eV at room temperature.

The full-width resolution of the spectral peak was 1.5 eV. The energy resolution was 2 percent of the pass energy, that is, 0.5 eV. The peak maxima could be

located to  $\pm 0.1$  eV. The reproducibility of peak height was good, and the probable error in the peak heights ranged from  $\pm 2$  percent to  $\pm 8$  percent.

### Friction Experiments

**In ultra-high-vacuum system.**—In situ friction experiments were conducted with the surface-treated foil specimens at temperatures from room temperature to 350° C. A load of 0.2 N was applied to the pin-flat contact. To obtain consistent experimental conditions, contact before sliding was maintained for 30 sec. Both the load and friction force were continuously monitored during a friction experiment. Sliding velocity was 0.05 mm/sec over a total sliding distance of 0.03 to 0.05 m. These experiments were single-pass sliding.

All friction experiments were conducted in a 10-nPa vacuum. The coefficients of friction reported herein were obtained by averaging three to five measurements. The maximum standard deviations of the data were within  $\pm 4$  percent of the average value.

Friction traces were primarily characterized by randomly fluctuating behavior with occasional evidence

of stick-slip behavior over the entire temperature range. The average coefficient of friction in the investigation was calculated from maximum peak heights in the friction trace resulting from a single-pass sliding of the sapphire rider.

**In argon atmosphere.**—The foils of the metallic glasses and the rider specimen surfaces were scrubbed with levigated alumina, rinsed with tap water and then with distilled water, and finally rinsed with ethyl alcohol. After the surface was dried with argon gas, the specimens were placed into the experimental apparatus. The specimen surfaces were then brought into contact and loaded, and the friction experiment was begun.

## Results and Discussion

### X-Ray Photoelectron Spectra

**Fe<sub>67</sub>Co<sub>18</sub>B<sub>14</sub>Si<sub>1</sub> alloy.**—The XPS spectra of the Fe<sub>2p</sub>, Co<sub>2p</sub>, B<sub>1s</sub>, Si<sub>2p</sub>, and C<sub>1s</sub> obtained from narrow scans on the Fe<sub>67</sub>Co<sub>18</sub>B<sub>14</sub>Si<sub>1</sub> foil surface are presented in figure 3. After bakeout the as-received foil was argon ion

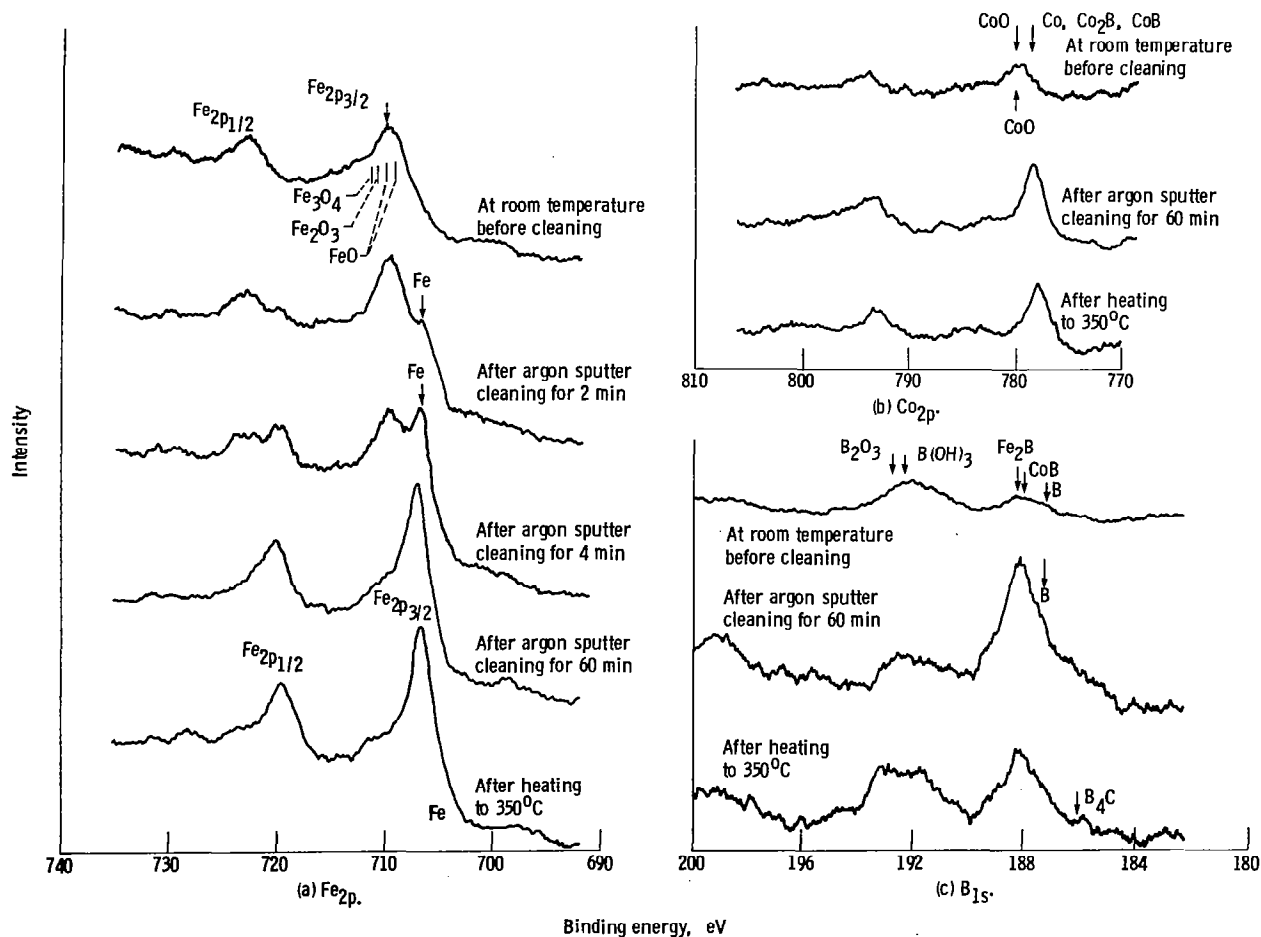


Figure 3. - Representative Fe<sub>2p</sub>, Co<sub>2p</sub>, B<sub>1s</sub>, Si<sub>2p</sub>, and C<sub>1s</sub> XPS peaks on Fe<sub>67</sub>Co<sub>18</sub>B<sub>14</sub>Si<sub>1</sub> surface.

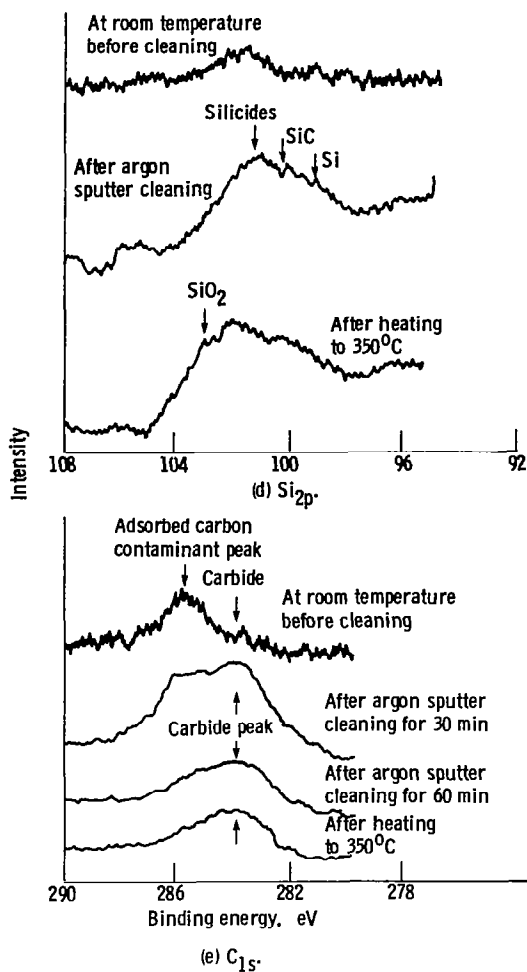


Figure 3. - Concluded.

bombarded and then heated at various temperatures in a 10-nPa vacuum. All the XPS spectra were taken at room temperature.

The  $Fe_{2p}$  peaks of the as-received specimen are shown in figure 3(a). The results clearly indicate that there were iron oxides on the foil surface. The spectra taken after the foil surface had been argon sputter cleaned for 2 and 4 min reveal that the lines for  $Fe_{2p}$  were split asymmetrically into doublet peaks. The doublet peaks are associated with iron oxide. The spectra taken after the foil surface had been argon sputter cleaned for 30 and 60 min clearly indicate the  $Fe_{2p}$  peaks associated with iron. The iron oxide peak is very small. The spectrum for the foil heated to 350° C is almost the same as that for the surfaces that had been argon sputter cleaned for 30 and 60 min.

The  $Co_{2p}$  peaks (fig. 3(b)) of the as-received specimen indicate cobalt oxide at 780 eV. The spectra for the surfaces that had been argon sputter cleaned and heated

to 350° C reveal only peaks for cobalt and its alloy. The cobalt oxide peak is negligible.

The  $B_{1s}$  peak of the as-received specimen (fig. 3(c)) suggests the presence of boric oxides as well as  $Fe_2B$ ,  $CoB$ , and  $B$ . The spectrum of the surface that had been argon sputter cleaned reveals higher peaks for boron and its alloys as well as very small boric oxide peaks. The spectrum for the foil heated to 350° C clearly indicates that the foil surface was again contaminated with boric oxides that had migrated from the foil specimen bulk. It is anticipated from these results that the tribological properties of the as-received foil at high temperatures would be different from those for the argon-sputter-cleaned surface.

The  $Si_{2p}$  peak of the as-received surface (fig. 3(d)) reveals silicides. The spectrum of the surface that had been argon sputter cleaned also reveals silicides, although there were silicon oxides as well as silicides on the surface. The foil heated to 350° C was contaminated with the silicon oxide that had migrated from the foil specimen bulk.

Photoelectron lines for the  $C_{1s}$  of the foil are shown in figure 3(e). An adsorbed carbon contaminant peak is evident in the spectrum for the as-received specimen. The doublet peaks of the surface that had been argon sputter cleaned for 30 min were due to the distinguishable kinds of carbon, that is, (1) a carbon contamination peak and (2) a carbide peak. The spectra of the surface that had been argon sputter cleaned for 60 min and of the surface heated to 350° C indicate a small carbide peak. Although the  $Fe_{67}Co_{18}B_{14}Si_1$  foil was not supposed to include carbon, carbides were present in the foil.

Table II summarizes the surface conditions of the foils analyzed by XPS. Generally the XPS results indicate that the surface of the as-received  $Fe_{67}Co_{18}B_{14}Si_1$  foil consisted of a layer of oxides of iron, cobalt, boron, and silicon as well as a simple, adsorbed film of oxygen and carbon. The argon-sputter-cleaned surface consisted of iron, cobalt, boron, silicon, and carbon. The surface heated to 350° C primarily consisted of a layer of the alloy, boric oxide, and silicon oxide.

**$Fe_{81}B_{13.5}Si_{3.5}C_2$ .** - The XPS spectra obtained from the foil surface are presented in figure 4. The surface condition of the foil was basically the same as that for  $Fe_{67}Co_{18}B_{14}Si_1$  already mentioned. The surface conditions are summarized in table II. Generally the surface of the as-received  $Fe_{81}B_{13.5}Si_{3.5}C_2$  foil contained a layer of the oxides or iron, boron, silicon, and carbon as well as a simple adsorbed film of oxygen and carbon. The argon-sputter-cleaned surface consisted of the alloy and small amounts of oxides. The surface heated to 350° C contained primarily the metallic element constituents as well as boric and silicon oxides.

**$Fe_{40}Ni_{38}Mo_4B_{18}$ .** - The surface condition of the  $Fe_{40}Ni_{38}Mo_4B_{18}$  foil was basically the same as those for

TABLE II. – SURFACE OF METALLIC GLASSES

Alloy composition	Surface		
	As received	Argon sputter cleaned	Heated to 350° C
$Fe_{67}Co_{18}B_{14}Si_1$	Oxides of Fe, Co, B, Si, and C Adsorbed film of oxygen and carbon	Alloy Small amount of oxides	Alloy Boric oxides and silicon oxides migrated from bulk
$Fe_{81}B_{13.5}Si_{3.5}C_2$	Oxides of Fe, B, Si, and C Adsorbed film of oxygen and carbon	Alloy Small amount of oxides	Alloy Boric oxides and silicon oxide migrated from bulk
$Fe_{40}Ni_{38}Mo_4B_{18}$	Oxides of Fe, B, Ni, Mo, and B Adsorbed film of oxygen and carbon	Alloy Small amount of oxide	Alloy Boric oxides migrated from bulk

$Fe_{67}Co_{18}B_{14}Si_1$  and  $Fe_{81}B_{13.5}Si_{3.5}C_2$  and is summarized in table II.

### Friction

**Vacuum.** – Sliding friction experiments were conducted with the  $Fe_{67}Co_{18}B_{14}Si_1$ ,  $Fe_{81}B_{13.5}Si_{3.5}C_2$ , and  $Fe_{40}Ni_{38}Mo_4B_{18}$  foils in contact with an aluminum oxide spherical rider at temperatures to 350° C and a pressure of 10 nPa. Contact was held for 30 sec before sliding in order to maintain the same experimental conditions. The coefficient of friction as a function of temperature is shown in figure 5. The foils and riders were sputter cleaned at room temperature and then heated. The coefficient of friction generally increased with increasing temperature from 1.4 for  $Fe_{67}Co_{18}B_{14}Si_1$  and 1.0 for  $Fe_{81}B_{13.5}Si_{3.5}C_2$  at room temperature to 2.2 and 1.7, respectively, at 350° C. Although the coefficient of friction remained low below 250° C, it increased rapidly with increasing temperature in the range 250° to 350° C. The rapid increase in friction from 250° to 350° C may be attributed to an increase in adhesion resulting (1) from crystallization of the foil and (2) from the segregation of boric oxide and silicon oxide to the surface of the alloy.

The experiments herein started with a surface that was nearly amorphous but contained very small crystallites (a few nanometers in diameter). Crystallization occurs with increasing temperature. Crystallized foils are less resistant to adhesion and plastic flow than are amorphous surfaces. There are many examples showing that the surface energy of a polycrystalline material is higher than that of an amorphous material. The general increase in friction at high temperatures may then be partly due to the increased adhesion and plastic flow in the contact area.

As already mentioned, at 350° C the foil surface was contaminated with boric oxide and silicon dioxide that had migrated from the foil specimen bulk to the surface. The oxide-to-oxide ( $Al_2O_3$  rider) interactions produce stronger bonding than does the oxide-to-metal interaction (refs. 5 and 6). The increase in friction at high temperatures is due to increased adhesion, that is, the increased bonding associated with oxidation of the foil surface. Thus there are two possible mechanisms for increasing adhesion. The first mechanism involves the crystallization process, and the second the bond strength of the oxides. In the absence of surface oxides only the crystallization process plays a role in increasing adhesion.

**Argon.** – Sliding friction experiments were conducted in argon with normal residual surface oxides present on the amorphous  $Fe_{67}Co_{18}B_{14}Si_1$  over a range of loads. The results obtained in these experiments are presented in figure 6. Although at a very light load of 0.01 N the coefficient of friction was extremely high, it decreased with increasing load to 0.35 at 0.02 N and remained there.

To determine the effect of the presence or absence of crystallinity on friction behavior, foils were heated to 650° C for 2 hr in a vacuum furnace, cooled to room temperature, cleaned as prescribed in the experimental procedure, and then examined in a friction experiment. The results obtained are presented in figure 6 together with those already described for the metal in the amorphous state. At all loads in figure 6, the coefficient of friction for the alloy in the amorphous state was less than it was for the same alloy in the crystalline state. Thus the absence of crystallinity resulted in lower friction.

There was a complete absence of any visible wear track on the amorphous foil, but a wear track was visible on the crystallized surface. The amount of surface oxide was

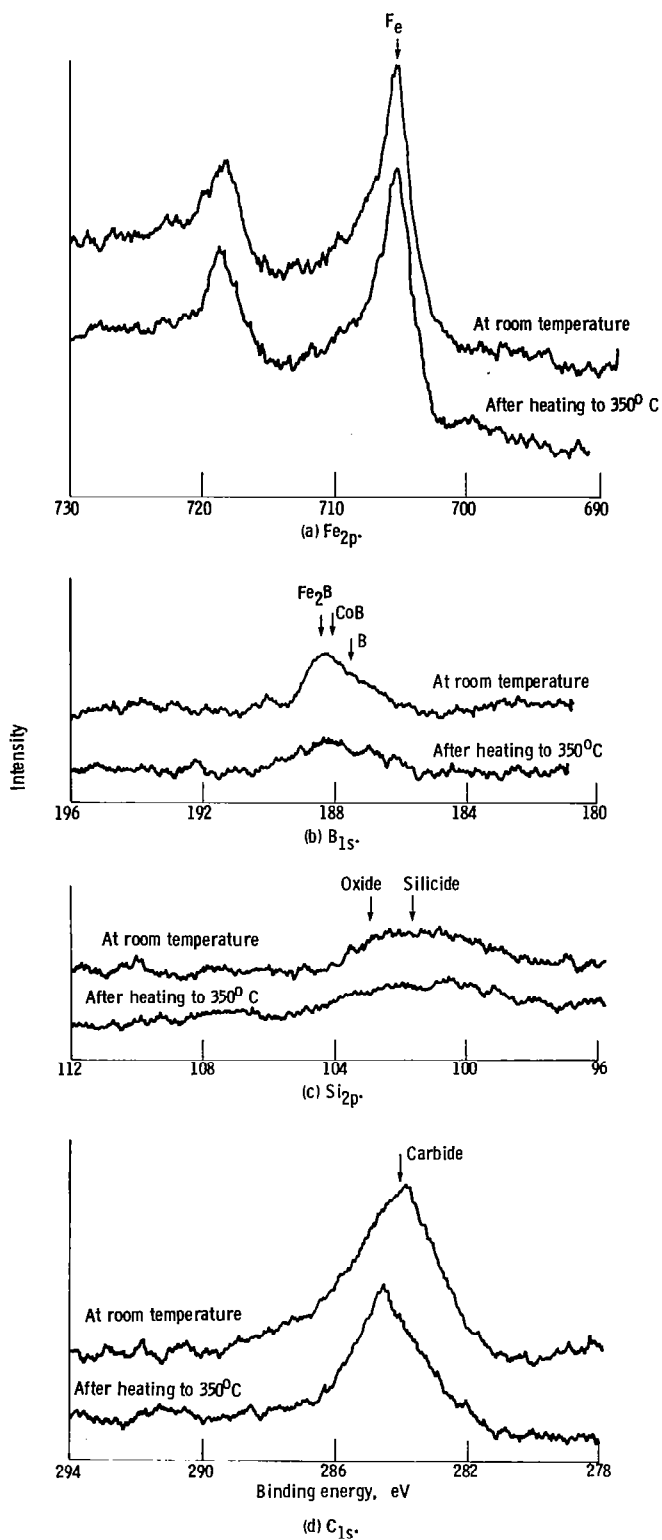


Figure 4. - Representative  $Fe_{2p}$ ,  $B_{1s}$ ,  $Si_{2p}$ ,  $C_{1s}$  XPS peaks on  $Fe_{81}B_{13.5}Si_{3.5}C_2$  surface.

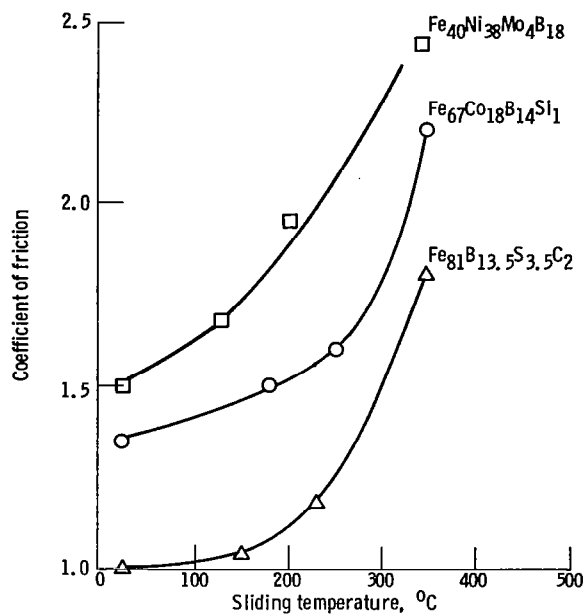


Figure 5. - Coefficient of friction as a function of temperature for aluminum oxide sliding on  $Fe_{40}Ni_{38}Mo_4B_{18}$ ,  $Fe_{67}Co_{18}B_{14}Si_1$ , and  $Fe_{81}B_{13.5}Si_{3.5}C_2$  alloys in vacuum. Normal load, 0.2 N; sliding velocity, 0.05 mm/sec; vacuum,  $10^{-8}$  Pa; sputter-cleaned foils.

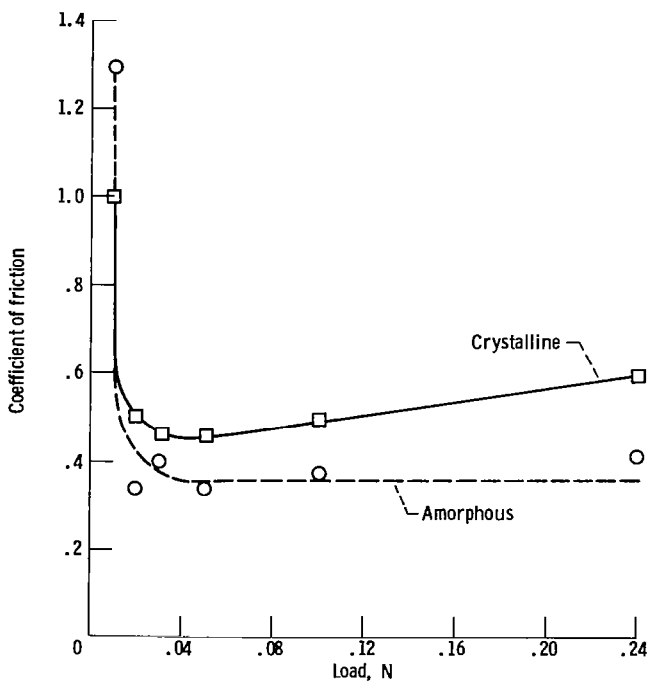


Figure 6. - Coefficient of friction as a function of load for aluminum oxide sliding on  $Fe_{67}Co_{18}B_{14}Si_1$  alloy in argon. Sliding velocity, 0.3 mm/sec.

greater in the wear track of the crystalline sample. This is as might be anticipated since the crystalline surface would be a higher energy surface.

To establish the exact crystalline state of the foils used in the experiments of figure 6, transmission electron diffraction patterns were obtained on the as-received foils and the foils after having been subjected to heat treatment above the recrystallization temperature. The pattern for the as-received foil is presented in figure 7(a), and that for the foil annealed above the recrystallization temperature is presented in figure 7(b).

The pattern of figure 7(a) indicates that the foil was not completely amorphous but contained grains of approximately a few nanometers in diameter. The annealed foil shown in figure 7(b) had a general grain size after recrystallization of 0.3 to 1.0  $\mu\text{m}$ .

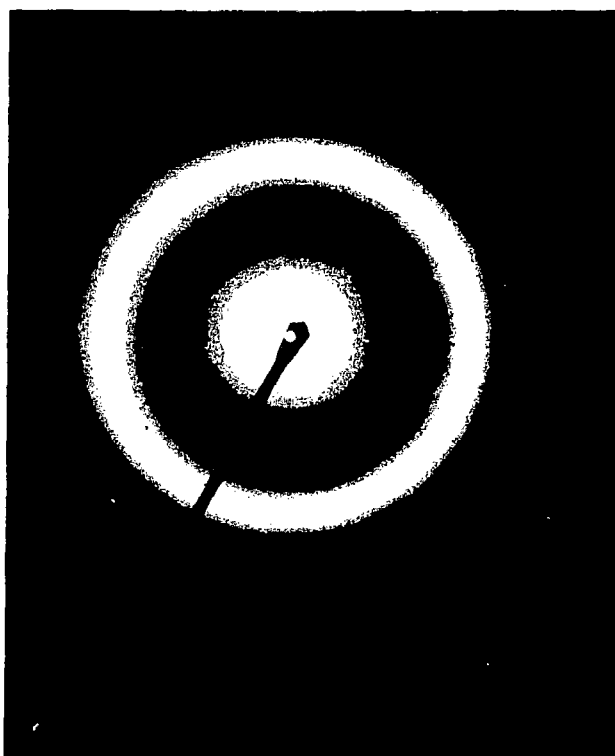
Since the alloy composition of figure 6 was a metallic glass, an obvious question would be, How does it compare in friction characteristics to conventionally used alloys? Therefore friction experiments were conducted with 304 stainless steel foils under conditions identical to those used in figure 6. The results obtained are presented in figure 8, where the dashed curve is for the amorphous alloy of figure 6.

From the data of figure 8 there appears to be very little difference in the friction behavior of the two alloys. In fact, at 0.01 N the 304 stainless steel exhibited lower friction. The wear results were, however, markedly different. As mentioned earlier, there was essentially no detectable wear on the surface of the amorphous alloy. There was, however, considerable wear to the 304 stainless steel surface as indicated by the photomicrograph of figure 9. Considerable plastic flow occurred and considerable oxide debris was generated on the 304 stainless steel. Lumps of metal appear in the wear track. Thus, while very little difference in the coefficient of friction was observed for the two alloys, marked differences in wear existed.

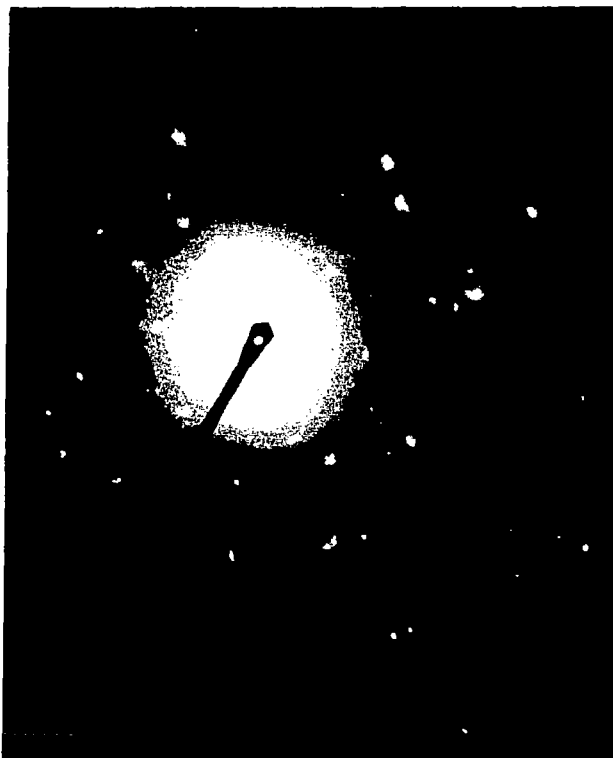
Variations in mechanical parameters such as sliding velocity do not appear to exert an effect on the friction behavior of the metallic glass, as indicated in the data of figure 10. In figure 10 over the range of sliding velocities from 0.03 to 1.6 mm/sec there was essentially no change in the coefficient of friction.

When the material in sliding contact with the amorphous alloy was something other than aluminum oxide, marked changes in friction behavior were observed. This is demonstrated in the data of figure 11, where copper and 52100 bearing steel were made to slide on the amorphous alloy. Both copper and 52100 in contact with the amorphous alloy resulted in greater friction than was observed with aluminum oxide (fig. 11).

Lubrication of the alloy surface with a conventional mineral oil reduced the friction for the alloy to levels comparable to those obtained with other metal alloys.



(a) As-received specimen; crystalline size, a few nanometers.



(b) Annealed specimen in vacuum at 0.2 to 0.3 Pa; crystalline size, 0.3 to 1  $\mu\text{m}$ ; annealing temperature, 650 $^{\circ}$  C; annealing time, 3 hr.

Figure 7. - Transmission electron diffraction patterns from thin foil as received and annealed. Acceleration voltage, 100 kV.

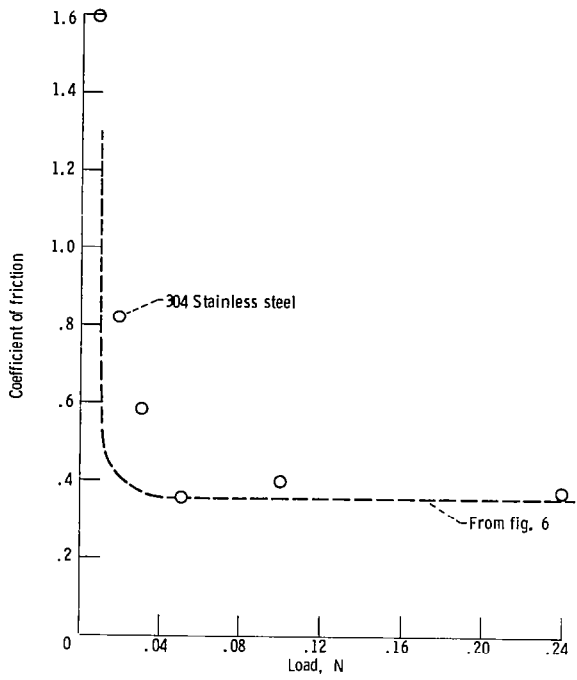


Figure 8. - Coefficient of friction as a function of load for aluminum oxide sliding on 304 stainless steel and  $Fe_{67}Co_{18}B_{14}Si_1$  alloy in argon. Sliding velocity, 0.3 mm/sec.

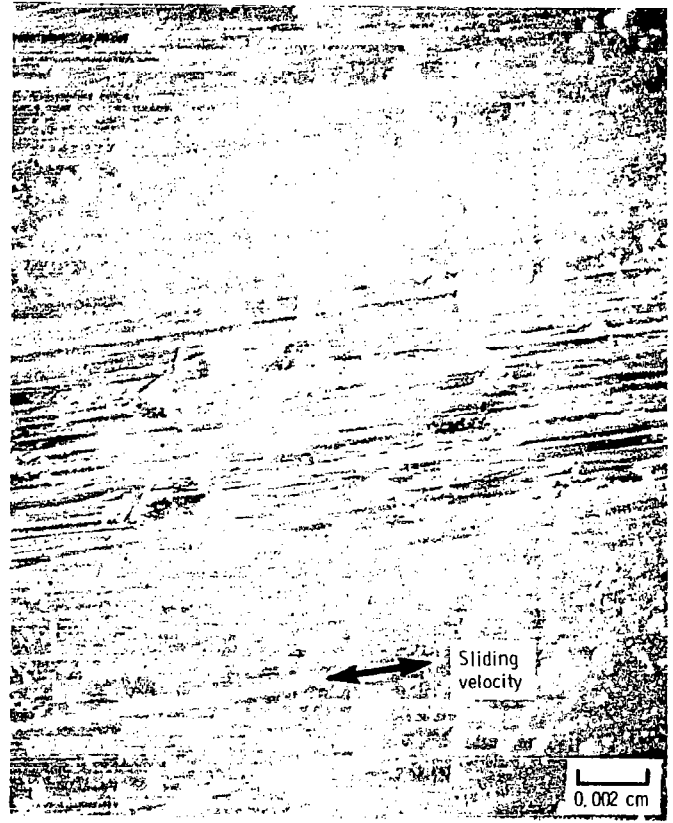


Figure 9. - Photomicrograph of 304 stainless steel wear surface. Rider, aluminum oxide; load, 0.01N; dry sliding in an argon atmosphere; sliding velocity, 0.3 mm/sec.

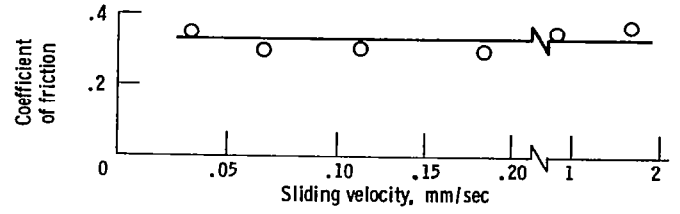


Figure 10. - Coefficient of friction as a function of sliding velocity for aluminum oxide sliding on  $Fe_{67}Co_{18}B_{14}Si_1$  amorphous alloy in argon. Dry sliding; normal load, 0.1 N; room temperature.

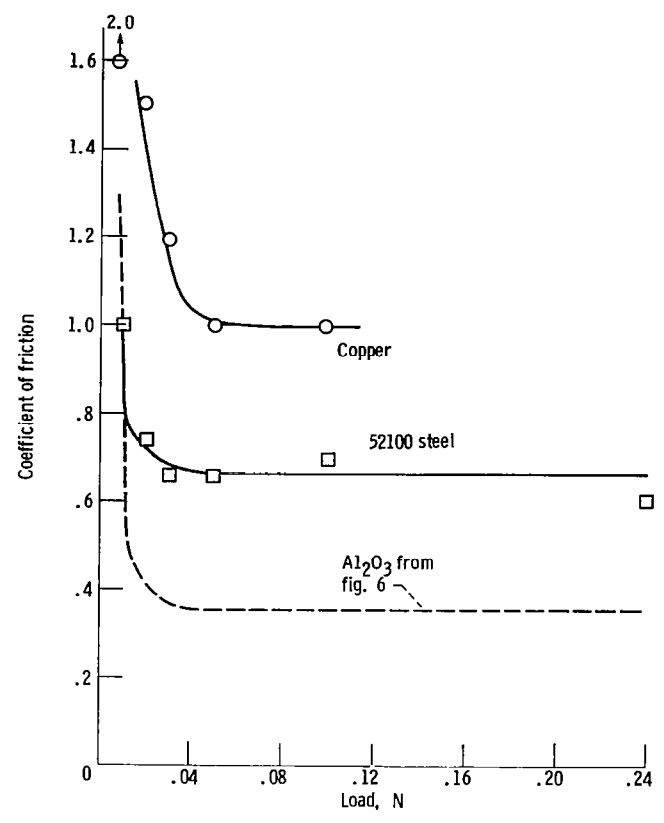


Figure 11. - Coefficient of friction as a function of load for various riders sliding on  $Fe_{67}Co_{18}B_{14}Si_1$  amorphous alloy in argon. Sliding velocity, 2.0 cm/min; room temperature.

This is indicated in the data of figure 12, where beyond a load of 0.05 N the coefficient of friction is 0.1. This is consistent with the boundary lubrication of metallic alloys by mineral oils.

The friction track for the alloy lubricated with mineral oil was extremely smooth whether the mating rider was aluminum oxide, 52100 bearing steel, or copper. Microscopic examination of the alloy surface showed no visible evidence for adhesion. The mean track was extremely smooth, with the surface having a polished appearance. This polished appearance may have resulted from the presence of surface oxide. In dry sliding these oxides were visible on the alloy surface. However, in the

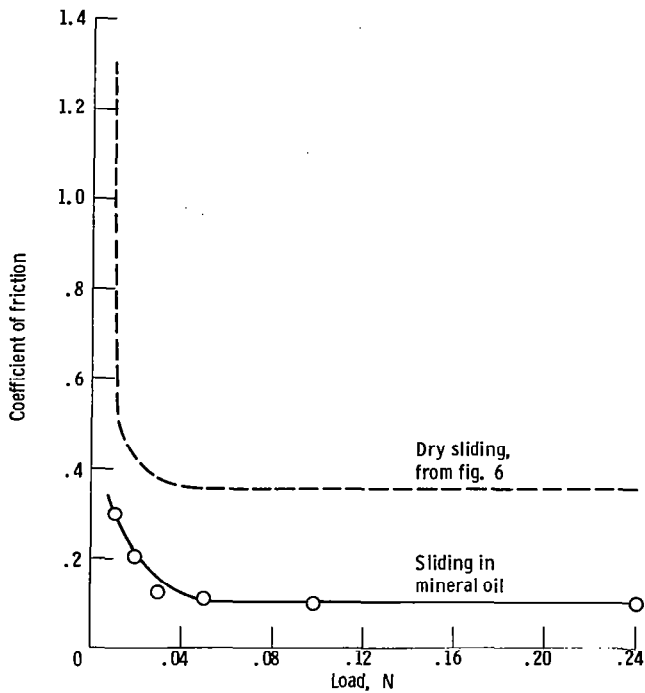


Figure 12. - Coefficient of friction as a function of load for aluminum oxide sliding on  $Fe_{67}Co_{18}B_{14}Si_1$  amorphous alloy in argon. Sliding velocity, 2.0 cm/min; room temperature.



Figure 14. - Photomicrograph of wear track on  $Fe_{81}B_{13.5}Si_{3.5}C_2$  amorphous alloy surface. Rider, aluminum oxide; load, 0.1N; dry sliding in argon; sliding velocity, 0.3 mm/sec.

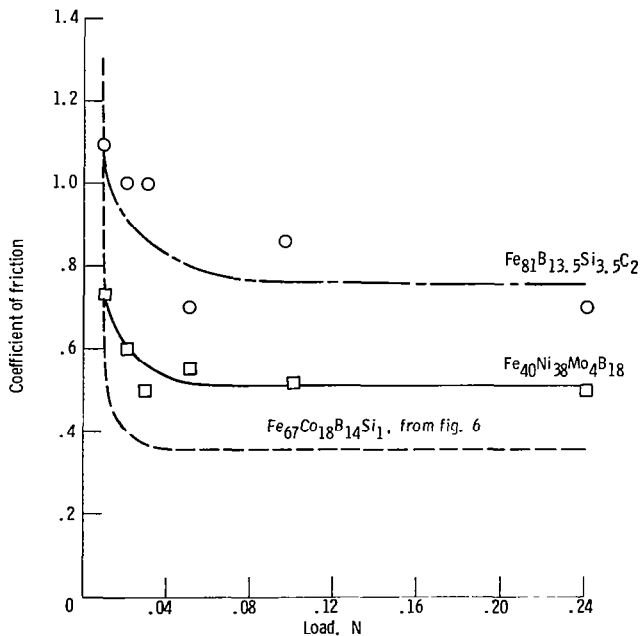


Figure 13. - Coefficient of friction as a function of load for aluminum oxide sliding on amorphous alloys in argon. Sliding velocity, 2.0 cm/min; room temperature.

mineral oil they were swept out of the contact zone. Their hard nature and small particle size makes a fine abrasive and therefore a good surface-polishing agent.

Marked differences can exist among the friction properties of amorphous alloys. As stated in the Introduction, there are many compositions that can form amorphous or glassy structures. Two alloys in the glassy state were examined in addition to  $Fe_{67}Co_{18}B_{14}Si_1$ . These alloys were also ferrous-base materials. Friction data obtained with these alloys are presented in figure 13. There is a considerable difference in the friction measured for the variations in alloy chemistry.

Figure 14 is a photomicrograph of the wear scar generated on the surface of the  $Fe_{81}B_{13.5}Si_{3.5}C_2$  alloy. Very little surface damage occurred despite the high friction forces measured with this alloy.

## Conclusions

As a result of sliding friction experiments conducted in this investigation with ferrous-base metallic glasses in contact with aluminum oxide in vacuum and in argon at

atmospheric pressure, the following conclusions were drawn:

1. The coefficient of friction increased with increasing temperature in vacuum. The increase in friction is believed to be due primarily to formation of boric oxide and silicon oxide by diffusion to the surface of the metallic glass.

2. The physical conclusion from the surface analysis is that the surfaces of metallic glasses oxidize significantly. Even cleaning surfaces very carefully inside a vacuum chamber, where such techniques as ion bombardment are used to remove oxides and adsorbed layers, may not necessarily produce a clean surface. The contaminant can come from within the bulk of the material and impart boric oxide and silicon oxide films on the solid surface with heating to 350° C.

3. The friction coefficients of the metallic glasses in argon increased with the crystallization of the alloys.

4. Different ferrous-base metallic glasses were examined and were found to have markedly different friction characteristics.

Lewis Research Center  
National Aeronautics and Space Administration  
Cleveland, Ohio, October 30, 1981

## References

1. Jones, H.: Splat Cooling and Metastable Phases. *Rep. Prog. Phys.* vol. 36, 1978, pp. 1425-1497.
2. Gilman, John J.: Metallic Glasses. *Physics Today*, vol. 28, no. 5, May 1975, pp. 46-53.
3. Gilman, J. J.: Metallic Glasses—A New Technology. Chapter 111.1, *Crystal Growth and Materials: Review Papers of the First European Conference on Crystal Growth ECCG-1, Zurich, Sept. 1976*, E. Kaldis and H. J. Scheel, eds., Current Topics in Materials Science, vol. 2, Elsevier-North Holland Publishing Co., 1977, pp. 728-741.
4. DeCristofaro, N.; and Henschel, C.: Matglas Brazing Foil. *Welding Journal*, vol. 57, no. 7, July, 1978, pp. 33-38.
5. Pepper, S. V.: Effect of Interfacial Species on Shear Strength of Metal-Sapphire Contact. *J. Appl. Phys.*, vol. 50, no. 12, Dec. 1979, pp. 8062-8065.
6. Miyoshi, Kazuhisa; and Buckley, Donald H.: The Effect of Oxygen and Nitrogen Interactions on Friction of Single-Crystal Silicon Carbide. NASA TP-1265, 1978.

1. Report No. NASA TP-1991	2. Government Accession No.	3. Recipient's Catalog No.	
4. Title and Subtitle <b>FRICION AND SURFACE CHEMISTRY OF SOME FERROUS-BASE METALLIC GLASSES</b>		5. Report Date March 1982	6. Performing Organization Code <b>506-53-12</b>
		8. Performing Organization Report No. <b>E-919</b>	10. Work Unit No.
7. Author(s) Kazuhisa Miyoshi and Donald H. Buckley		11. Contract or Grant No.	
9. Performing Organization Name and Address Lewis Research Center National Aeronautics and Space Administration Cleveland, Ohio 44135		13. Type of Report and Period Covered <b>Technical Paper</b>	
		14. Sponsoring Agency Code	
12. Sponsoring Agency Name and Address National Aeronautics and Space Administration Washington, D. C. 20546		15. Supplementary Notes	
16. Abstract <p>The friction properties of some ferrous-base metallic glasses were measured both in argon and in vacuum to a temperature of 350<sup>o</sup> C. The alloy surfaces were also analyzed with XPS (X-ray photoelectron spectroscopy) to identify the compounds and elements present on the surface. The results of the investigation indicate that even when the surfaces of the "amorphous" alloys, or metallic glasses, are atomically clean, bulk contaminants such as boric oxide and silicon dioxide will diffuse to the surfaces. Friction measurements in both argon and vacuum indicate that the alloys exhibit higher coefficients of friction in the crystalline state than they do in the amorphous (glassy) state.</p>			
17. Key Words (Suggested by Author(s)) Metallic glasses X-ray photoelectron spectroscopy Friction		18. Distribution Statement Unclassified - unlimited STAR Category 26	
19. Security Classif. (of this report) Unclassified	20. Security Classif. (of this page) Unclassified	21. No. of Pages 13	22. Price* A02